2

Strain Measurements Relative to Normal State Enhance the Ability to Detect Non-Transmural Myocardial Infarction

Noa Bachner-Hinenzon[1,*], Offir Ertracht[2, 3,*], Zvi Vered[4,5], Marina Leitman[4,5], Nir Zagury[1], Ofer Binah[2,3] and Dan Adam[1]
[1]*Faculty of Biomedical Engineering*
[2]*Department of Physiology*
[3]*Ruth and Bruce Rappaport Faculty of Medicine, Rappaport Family Institute for Research in the Medical Sciences Technion-Israel Institute of Technology, Haifa,*
[4]*Department of Cardiology, Assaf Harofeh Medical Center, Zerifin,*
[5]*Sackler School of Medicine Tel Aviv University*
Israel

1. Introduction

Nowadays, diagnosis of heart pathologies in the clinic is mostly performed non-invasively by eyeballing the B-mode echocardiography cines and evaluating the ejection fraction and the regional wall motion. Yet, myocardial infarction (MI) usually causes reduced regional wall motion. During its diagnosis the echocardiographer grades the movement of each myocardial segment in order to estimate its function (Schiller et al., 1989). The disadvantage in this estimation is that it is subjective, and the echocardiographer must be experienced (Picano et al., 1991). As a result, echocardiographers provide different scoring to the same patient (Liel-Cohen et al., 2010). Hence, major efforts are invested in constructing automatic tools for wall motion estimation, as Speckle Tracking Echocardiography (STE).

The STE is an angle-independent, cost-effective and available tool, developed for automatic evaluation of left ventricular (LV) regional function (Leitman et al., 2004, Liel-Cohen et al., 2010, Reisner et al., 2004). The STE program processes standard echocardiographic two dimensional (2D) gray-scale cine loops and tracks the speckle movement frame-by-frame (Rappaport et al., 2006). Consequently, the regional myocardial velocities are calculated and local strain parameters are provided. During MI, these local strain parameters, calculated in the longitudinal, circumferential and radial orientations, were found to be strongly correlated to MI size (Fu et al., 2009, Gjesdal et al., 2007, 2008, Migrino et al., 2007, 2008). Furthermore, the detection of large MI was found to be very reliable (Gjesdal et al., 2008, Migrino et al., 2007). Yet, the detection of small non-transmural MI requires improvement. Since it is important to achieve early detection of non-transmural MI, in the present study we investigated the

[*]These authors contributed equally to the manuscript

hypothesis that taking into consideration the natural heterogeneity of the strain measurements among the different segments would enhance the differentiation between non-transmural MI and non-MI areas. This kind of measurement is particularly suitable for stress-echocardiography since this prevalent clinical study includes comparison of the echo results at stress to those at baseline, and is specified for the detection of minor ischemia.

In this study 13 rats in the acute phase of MI (24 hours) and 8 sham operated rats were scanned, and their short axis cines were analyzed by a STE program. Subsequently, the Radial Strain (S_R) and Circumferential Strain (S_C) were evaluated at 6 myocardial segments. The first step was to decipher the natural heterogeneity at normal state by measuring the peak systolic strain values for each segment averaged over the 21 rats. The second step was to measure the segmental peak systolic strain values conventionally and relatively to normal state. Subsequently, the strain values were compared to the MI size and location.

2. Methods

Animal experiments were conducted according to the institutional animal ethical committee guidelines (ethics number: IL-101-10-2007) in 3 month old adult male Sprague-Dawley rats weighing 310-340 gr. Rats were maintained at the Experimental Surgical Unit of the Technion, and fed on normal rodent chow diet, with tap water ad libitum, according to the Technion guidelines for animal care. The rats were housed at a constant temperature (21°C) and relative humidity (60%) under a regular light/dark schedule (light 6:00 AM to 6:00 PM).

In this study 21 adult male Sprague-Dawley rats were investigated. Thirteen rats underwent myocardial ischemia and reperfusion surgery and 8 rats served as a corresponding sham group.

2.1 Surgical procedure

Male Sprague-Dawley rats were randomly divided into 2 groups. All rats were anesthetized with a combination of 87 mg/kg ketamine and 13 mg/kg xylazine mixture. The animals were intubated and mechanically ventilated using a Columbus Instruments small-animal mechanical respirator (Columbus Instruments 950 North Hague Av. Columbus, OH. USA) at a rate of 80-90 cycles per minute with a tidal volume of 1-2 ml/100 gr. Using a left thoracotomy, the chest was opened, the pericardial sac dissected, and the heart exposed. A single stitch was placed through the myocardium at a depth slightly greater than the perceived level of the left anterior descending artery (LAD) while taking care not to puncture the ventricular chamber (Bhindi et al., 2006, Hale et al., 2005). In the first group, which included 13 rats, the suture was tightened by a loop that allowed its rapid opening. Half an hour after the occlusion the suture was rapidly opened in order to resume blood flow through the LAD. In the second group, which included 8 rats, the thread was placed through the myocardium but it was not tied up; however, the chest remained opened for half an hour. Finally, the chest was closed and the animal was allowed to recover.

2.2 Echocardiographic measurements

Echocardiographic transthoratic scans were performed at baseline and at 24 hours of reperfusion. For the baseline and 24 hours post-MI echocardiographic scans, animals were

lightly sedated by an intraperitoneal injection of 29 mg/kg ketamine and 4.3 mg/kg xylazine mixture. Their chest was shaved and the scan was performed. During the scan, rats were placed in a left lateral decubitus position. The scan was performed via a commercially available echo-scanner - Vivid™ *i* ultrasound cardiovascular system (GE Healthcare Inc. Israel) using a 10S phased array pediatric transducer and a cardiac application. The transmission frequency was 10 MHz, the depth was 2.5 cm and the frame rate was 225-350 frames per second. The measurements included 2 short axis cross-sections at the Apical (AP) level and the Papillary Muscles (PM) level.

2.3 Speckle tracking echocardiography

The short axis ultrasound cines were post-processed by an enhanced STE program that measures the regional LV function at 6 segments with high spatial resolution (Bachner-Hinenzon et al., 2010, 2011). The program utilizes a commercial STE program called '2D-strain' (EchoPAC Dimension '08, GE Healthcare Inc., Norway). The commercial program requests the user to mark the endocardial border and to choose the width of the myocardium, imposes a grid of points in the assigned region, and tracks the speckles near the points and evaluates their velocities at each frame (Rappaport et al., 2006). The myocardial velocities were not processed by the built-in smoothing of the commercial program, but were de-noised by a 3D wavelet representation (MATLAB software, MathWorks Inc. USA), thereby increasing the spatial resolution of the calculated functional measurements (Bachner-Hinenzon et al., 2010). Subsequently, the Radial Strain (S_R) and Circumferential Strain (S_C) were evaluated at 6 segments. The strain parameters were measured from the de-noised velocities of each point on the grid. The S_R was calculated from the de-noised radial velocity, and the S_C and LV rotation were calculated from the de-noised circumferential velocity. Thereafter, the peak systolic values of the LV rotation S_R and S_C were calculated. The LV rotation is the rotation in degrees from the diastolic state. The S_C and S_R were measured in % from the diastolic state. End diastole is defined as the time just before the QRS complex in the ECG signal. The S_C and S_R were also calculated for each segment relatively to the normal values, as % of difference from the average baseline value divided by the average baseline value for each segment separately to create the 'S_C rel' and 'S_R rel'. For example, if the average normal strain was 14% at a specific segment, and the value decreased to 7%, the relative value was -50%.

2.4 Determination of MI size

The method used here for the assessment of the tissue viability, includes the use of two stains: (1) Evan's blue is used to delineate the Area At Risk (AAR), which is the area that was physically ligated 24 hours previously. (2) Triphenyltetrazolium Chloride (TTC), which delineates the MI area. Twenty four hrs post-surgery, the animals were re-anesthetized, intubated, and ventilated according to the protocol used in the surgery. The chest was opened to expose the heart. 1.5% Evan's blue solution (in PBS) was retrogradely injected through the aorta into the LV. The staining agent was then perfused through the open coronary arteries into the cardiac muscle, but not through the ligated artery and its downstream branches, delineating in dark blue the non-MI area of the heart. The heart was then removed and rinsed, in normal cold saline, of the excess Evan's blue and transferred to -80°C for 5-6 min and sliced manually into 7 transverse slices. The slices were dipped in 1% TTC solution (in DDW pH=7.4)

at 37°C for 20 min, and then rinsed in PBS of the excess TTC solution, and weighted (Ojha et al., 2008, Reinhardt et al., 1993). To improve the delineation of the different colours, the slices were kept at 4°C in PBS + sodium azide (0.01%), as preservative, for 3 weeks (Pitts et al., 2007). Subsequently, the slices were placed on top of a light table and photographed on both sides. Using the ImageJ software (NIH, Bethesda, MD, USA http://rsb.info.nih.gov/ij) the pictures were analyzed, and the different areas were delineated. Using the weights of the slices and the percentages of the different colored areas of each slice, we calculated the percent of non-MI cardiac muscle (dark blue), area at risk (red and white) and infarcted area (white). The slices were numbered from 1 to 7 from apex to atria. The slices that matched the AP and PM levels of short axis scans were slices number 3 and 4, respectively. These slices were divided to 6 equal radial segments: inferior septum, anterior septum, anterior wall, lateral wall, posterior wall and inferior wall. Each segment was classified as normal or damaged with transmural or non-transmural MI, according to the TTC stain.

2.5 Statistical analysis

All variables were expressed by the mean ± SEM. Paired t-test was performed in order to compare the MI size at the AP and PM levels. One-way analysis of variance (ANOVA) for unequal variance was used to compare MI size (normal/transmural/non-transmural) to the peak systolic strains (S_C, S_R, S_C rel, S_R rel). One-way ANOVA for unequal variance was also used in order to compare between the peak systolic strain of the different segments for the baseline and 24 hours of reperfusion results. Two-way repeated measures ANOVA was used to compare the peak systolic strains (S_C, S_R) at different time points for the MI and sham groups. Receiver operating characteristics (ROC) method was used in order to predict transmural MI from all other segments (normal and non-transmural). The ROC method was also used in order to predict non-transmural MI from the normal segments. The area under the ROC curves was measured and compared in order to test whether the difference between the ROC curves was significant.

3. Results

3.1 MI size

In 156 segments of the AP and PM levels of the 13 MI rats the determination of MI size by the TTC staining yielded the following results: 91 normal segments, 22 non-transmural MI and 43 transmural MI segments. The transmural MI occurred mostly at the anterior and lateral walls (in 10 out of 13 rats), while non-transmural MIs were visualized at the posterior and inferior walls (in 9 out of 13 rats). The total MI size at the AP level was 23±13 % (min 0%, max 47%), and at the PM level was 19±8 % (min 7%, max 34%), while there was no significant difference in the MI size between the two levels. The results for the sham group showed 86 normal segments for the 8 sham rats.

3.2 Strain measurements at baseline

Heterogeneity of the peak systolic strains was defined as a significant difference between the measured values at the different segments. Typical strain maps at the normal state, which are presented in Fig. 1A, illustrate the heterogeneity of the S_R and S_C. The average baseline values of S_C and S_R for 21 rats are presented in Fig. 1B and Fig. 1C, respectively. One way ANOVA test for the normal peak systolic S_C values demonstrate that the heterogeneity of the peak

systolic values at the AP level is significant (P<0.001), while this heterogeneity is no longer significant at the PM level (P=0.06, N.S). Yet, it can be seen that the pattern of the peak systolic S_C lines in Fig. 1B are similar for the AP and PM levels. One way ANOVA test for the peak systolic S_R values demonstrate that the heterogeneity of the peak systolic S_R is significant at both AP and PM levels (P<0.001). Both AP and PM levels show lower S_R at the inferior septum and anterior septum, and the values are higher for the lateral wall (P<0.05).

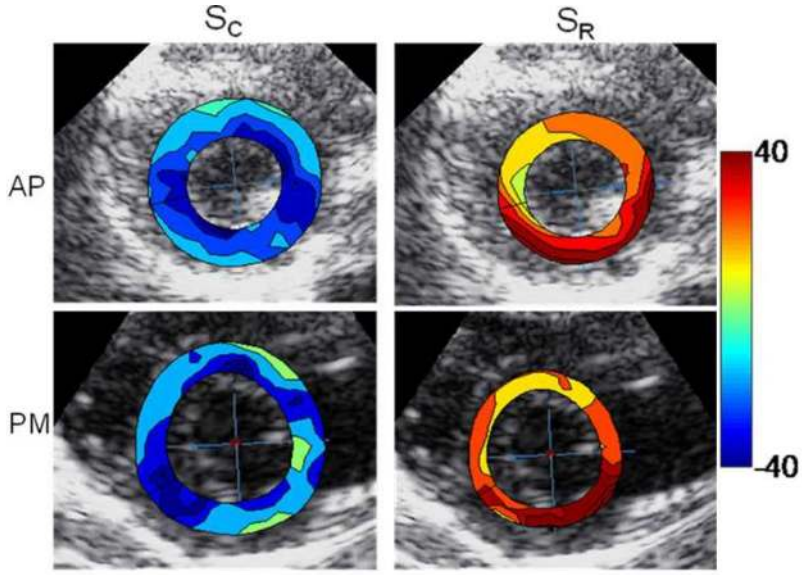

1A.

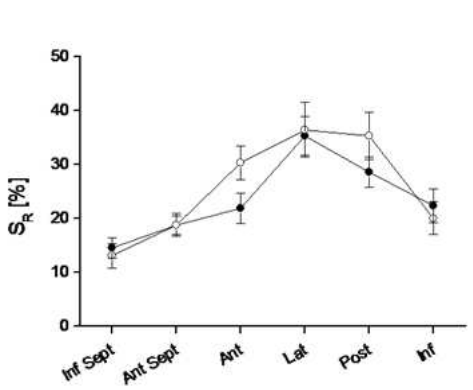

1B.

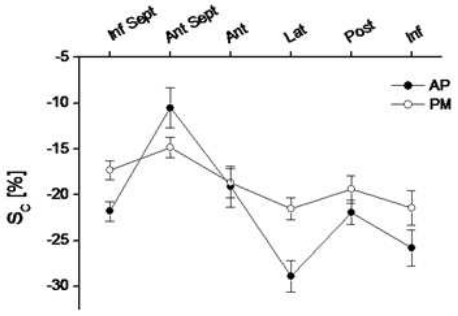

1C.

Fig. 1. The heterogeneity of normal strain values in % from diastolic state. Typical maps of end-systolic circumferential (S_C) and radial (S_R) strains at the apical (AP) and papillary muscles (PM) levels (1A). Blue color is defined as negative and red as positive. Peak systolic S_C (1B) and S_R (1C) at the different segments of the AP and PM levels averaged over 21 rats.

The global LV rotation was 4.9±0.5 deg counterclockwise at the AP level and 1.6±0.6 deg counterclockwise at the PM level.

3.3 Segmental strain measurements as function of time post-MI

Examples of strain maps of peak systolic values of S_C and S_R are depicted in Fig. 2 for slices of sham, non-transmural MI, and transmural MI. The changes in peak systolic S_C and S_R of both MI and sham groups at baseline and 24 hours of reperfusion are demonstrated in Fig. 3A-D. Twenty four hours after reperfusion, the peak systolic S_C and S_R were significantly decreased at the free wall in both AP and PM levels (Figs. 3A-D, $P<0.05$), while the septum maintained normal values.

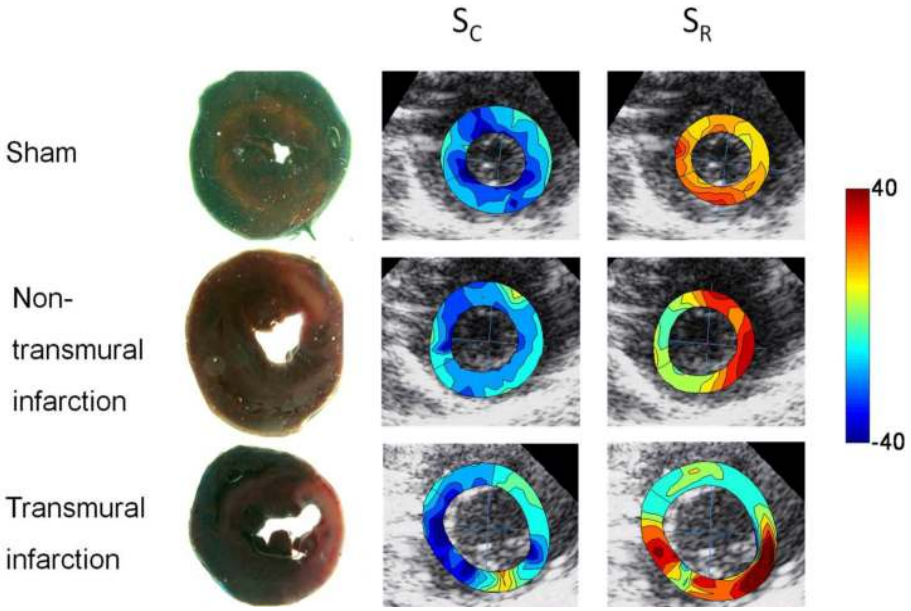

Fig. 2. Examples of TTC staining and end-systolic strain maps (% from diastolic state) for sham, non-transmural MI and transmural MI rats. Blue color is defined as negative and red as positive. In the example of sham rat it is well seen that the papillary muscles (PM) level is injured even though there was no LAD occlusion. In the non-transmural example, the yellow positive S_C is the MI area. This area looks rather normal in the S_R map. In the transmural example, green color of S_C is zero, and light blue of S_R is the thinning of the myocardium.

3.4 Strain measurements of MI rats versus sham rats

The peak systolic S_C values of the MI group decreased from normal values at the free wall of the AP and PM levels (Fig. 3A, 3C ,$P<0.05$). However, the peak systolic S_C values of the sham group decreased only at the lateral wall of the AP level (Fig. 3A, $P<0.05$), and posterior wall of the PM level (Fig. 3C, $P<0.01$), while there was no significant difference in the peak systolic S_C values between the MI and sham rats in these segments. The peak systolic S_C at the PM level maintained normal values for the sham group except for a slight reduction at the posterior wall (Fig. 3C, $P<0.01$).

The values of peak systolic S_R for the MI rats at the AP level at the anterior and lateral walls were smaller at 24 hours of reperfusion than baseline (Fig. 3B, $P<0.001$); however, the same reduction was noticed at the anterior wall of the sham group (Fig. 3B). Thus, only the peak systolic S_R of the lateral wall was significantly lower for the MI rats ($P<0.05$). At the PM level no significant difference was found in the peak systolic S_R between the sham group and the MI group (Fig. 3D). In both groups the peak systolic S_R became smaller at the lateral, posterior and inferior walls (Fig. 3D , $P<0.01$).

In both MI and sham groups, the LV rotation was depressed after surgery. Ten minutes after reperfusion, the LV apical rotations of the MI and sham groups were 0.2±0.4 deg and -1.1±1.4 deg, respectively. Twenty four hours after reperfusion, the LV rotations at the AP level of the MI and sham groups were 0.0±0.5 deg and -0.3±0.6 deg, respectively.

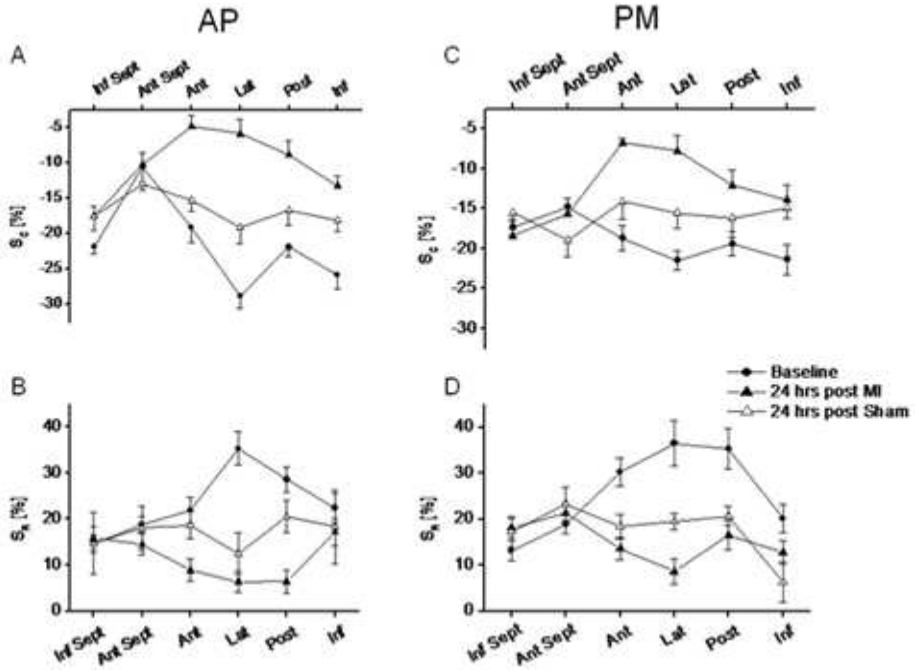

Fig. 3. Segmental circumferential strain (S_C) at the apical and papillary muscles levels as function of time (baseline and 24 hours of reperfusion) for the MI group and for the sham group (3A, 3C). Segmental radial strain (S_R) at the apical and papillary muscles levels as function of time for the MI group and for the sham group (3B, 3D).

3.5 Strain measurements versus MI size

Linear regression was performed between the MI size and the peak systolic S_C and S_R for both AP and PM levels. The linear regression was performed between the size of the MI (as % of area from the total area of the cross-section) and the peak systolic S_C and S_R averaged over the anterior, lateral and posterior segments of the same cross-section (MI area). Subsequently, the linear regression was performed between the cross-sectional MI size and

the peak systolic S_C and S_R averaged over the inferior septum, anterior septum and inferior wall (non-MI area). This analysis revealed high correlation between the MI size and the peak systolic strains of the MI area (Fig. 4). The correlation was higher at the AP level (S_C R2=0.89, S_R R2=0.73) than at the PM level (S_C R2=0.73, S_R R2=0.67) as seen in Fig. 4. In contrast, no correlation was found between the peak systolic S_C and S_R of the non-MI area and the MI size (AP: S_C R2=0.25, S_R R2=0.02, PM: S_C R2=0.00, S_R R2=0.05) (data not shown). Finally, there was no correlation between the peak systolic S_C and S_R of the MI area and the non-MI area (AP: S_C R2=0.27, S_R R2=0.06, PM: S_C R2=0.24, S_R R2=0.06); see discussion.

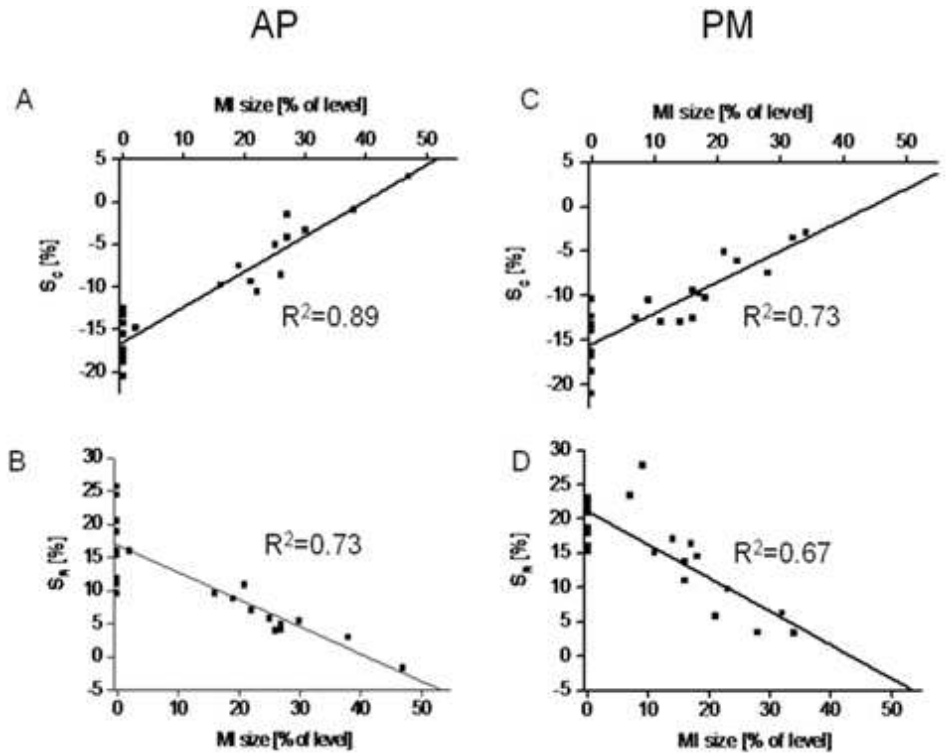

Fig. 4. Scatter plot and linear regression of apical peak systolic circumferential (S_C, 4A) and radial (S_R, 4B) strains versus MI size. Scatter plot and linear regression of peak systolic circumferential (S_C, 4C) and radial (S_R, 4D) strains at the papillary muscles level versus MI size. The strains are averaged over the anterior, lateral and posterior walls, and the MI size is measured per level.

Next, statistical analysis was performed to see whether there is a significant difference between the strain measurements of normal, non-transmural and transmural MI. As expected, segments with transmural MI demonstrated significantly lower peak systolic strain values than the normal segments in both AP and PM levels (Fig. 5, P<0.001). Furthermore, the segments with transmural MI could be distinguished from non-transmural MI segments by utilizing peak systolic S_C values as seen in Fig. 5A and Fig. 5E (AP P<0.01,

PM P<0.001). However, it was possible to do so with S_R values only at the PM level, as seen in Fig. 5F (P<0.01). The non-transmural MI segments could be distinguished from the normal segments at the PM level only by using peak systolic S_C values as seen in Fig. 5E (P<0.001), and not by using peak systolic S_R values (Fig. 5F). At the AP level it was impossible to distinguish the non-transmural MI segments from the normal segments by using peak systolic S_C and S_R as seen in Figs. 5A and 5B, respectively.

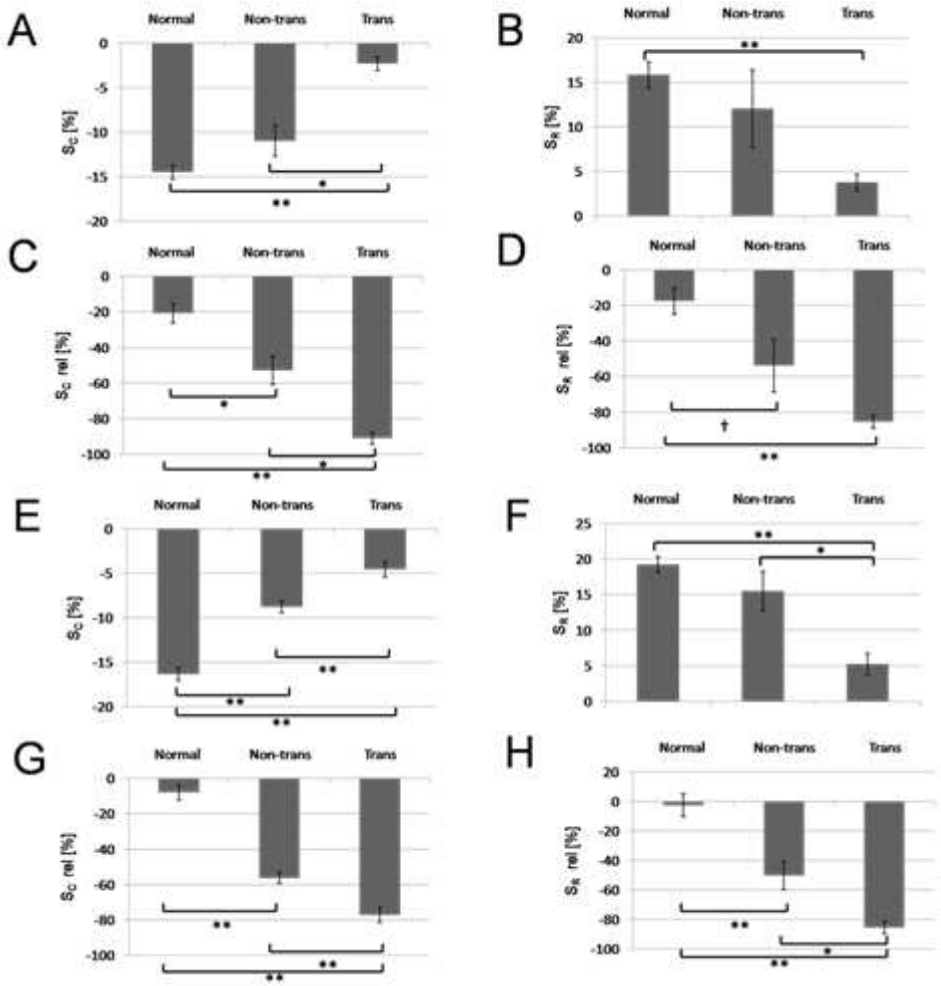

Fig. 5. Apical peak systolic circumferential (S_C, 5A) and radial (S_R, 5B) strains versus MI size (normal, transmural and non-transmural). Apical peak systolic circumferential (S_C rel, 5C) and radial (S_R rel, 5D) strains relative to normal state versus MI size. Peak systolic circumferential (S_C, 5E) and radial (S_R, 5F) strains at the papillary muscles level versus MI size. Peak systolic circumferential (S_C rel, 5G) and radial (S_R rel, 5H) strains relative to normal state at the papillary muscles level versus MI size. *P<0.01, **P<0.001, †P<0.05.

3.6 Strain measurements relative to normal state values

The peak systolic S_C and S_R relative to normal state values distinguished non-transmural MI from normal segments at the AP (Fig. 5C and Fig. 5D) and PM (Fig. 5G and Fig. 5H) levels (S_C rel P=0.01, S_R rel P<0.05, PM: S_C rel P<0.001, S_R rel P<0.001), while it was impossible at the AP level (Figs. 5A and 5B), and was possible at the PM level only by peak systolic S_C (Fig. 5E).

In order to compare between the peak systolic S_C and S_R and their values relative to normal state (peak systolic S_C rel and S_R rel) a ROC method was utilized and the areas under the curves were compared (Fig 6). The results are summarized in Table 1. In all cases the S_C relative to its normal state values provided the best results; however, in the detection of transmural MI, there is no significant difference between S_C relative to normal state and peak systolic S_C. The comparison between ROC curves, analyzing the detection of transmural MI at the AP level, appears in Fig. 6A. When studying the capabilities of detecting non-transmural MI, the S_C relative to its normal state values provided better results at the apex as seen in Fig. 6B (P<0.01), however, there was no significant difference in the capability of detection at the PM level. The detection of non-transmural MI by peak systolic S_R was enhanced by utilizing the measurement of peak systolic S_R relative to its normal state in both AP and PM levels. Nevertheless, at the PM level this detection was significantly less effective than the detection by peak systolic S_C as seen in Table 1 (P<0.05).

		Transmural MI		Non-transmural MI	
Parameter		AP	PM	AP	PM
S_C	Sensitivity	96 %, -7.5 %	100%, -9.4%	88%, -13.4%	100%, -13.4%
	Specificity	90%, -7.5 %	80%, -9.4%	65%, -13.4%	84%, -13.4%
S_R	Sensitivity	84%, 7.7%	81%, 7.5%	100%, 11.1%	57%, 10.3%
	Specificity	80%, 7.7%	98%, 7.5%	72%, 11.1%	89%, 10.3%
S_C rel	Sensitivity	**100%, -68.5%**	**100%, -56.9%**	**88%, -50.7%, ***	**100%, -41.1%**
	Specificity	**96%, -68.5%**	**83%, -56.9%**	**84%, -50.7%, ***	**87%, -41.1%**
S_R rel	Sensitivity	77%, -77.3%, †	82%, -77.3%	100%, -58.1%, *	64%, -48.5%, †
	Specificity	92%, -77.3%, †	97%, -77.3%	81%, -58.1%, *	84%, -48.5%, †

S_C and S_R are the peak systolic values. S_C rel and S_R rel are the peak systolic values relative to normal state. Specificity and sensitivity values appear on the left and their cut-off value appears on the right. Significant difference of ROC curves between the parameter and the parameter relative to normal state appears in the table as *P<0.01, † P<0.05.

Table 1. Specificity and sensitivity of peak systolic S_C and S_R

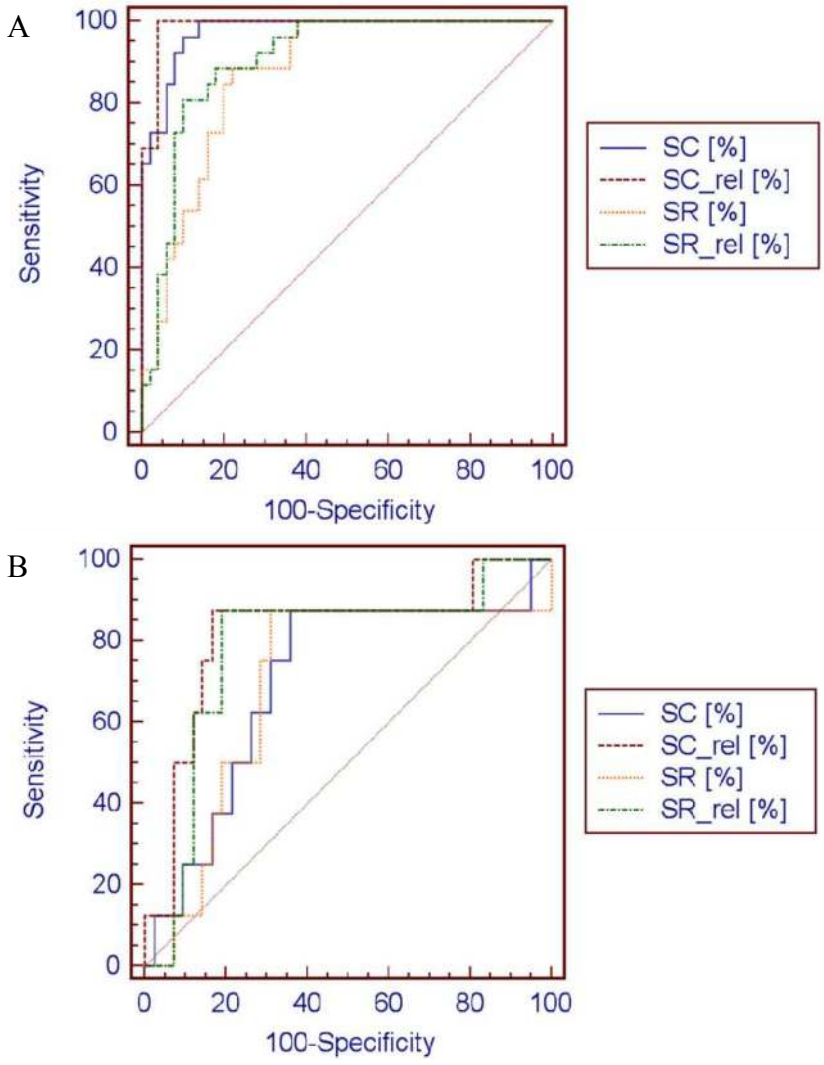

Fig. 6. Receiver operating characteristics curve of apical circumferential (S_C) and radial (S_R) strains and apical circumferential and radial strains relative to normal state (S_C rel, S_R rel) in the detection of transmural MI (6A) and non-transmural MI (6B). In the detection of non-transmural MI there is a significant difference between the S_C and S_R curves and the S_C rel and S_R rel curves ($P<0.01$).

4. Discussion

In the present study we tested the hypothesis that taking into consideration the natural heterogeneity of the strain measurements among the different segments would enhance the differentiation between non-transmural MI and non-MI areas. Our main findings were: 1) In normal rats, while peak systolic S_C is heterogeneous at the AP level, the heterogeneity is not statistically significant at the PM level. 2) In normal rats, peak systolic S_R is heterogeneous at both AP and PM short axis levels. 3) Peak systolic S_C is more sensitive to the presence of MI than peak systolic S_R. 4) Peak systolic S_C value, when calculated relatively to normal values (% of reduction from normal value) is more sensitive to the presence of non-transmural MI than the conventional peak systolic S_C value. 5) Peak systolic strains (S_C and S_R) at the MI areas have high correlation to MI size. 6) Peak systolic strains (S_C and S_R) at remote areas from the MI do not correlate to MI size. 7) Sham operated rats demonstrated lower strain values mostly at the anterior and lateral walls probably due to stunning of the myocardium due to the insertion of the needle (The needle was inserted and the thread was placed through the myocardium but it was not tied up). 8) LV apical rotation was severely depressed in both MI and sham rats.

In this study the heterogeneity of the peak systolic S_C and S_R was demonstrated in normal rats. Moreover, it was shown that this heterogeneity should be taken into account when attempting to detect non-transmural MI. When the normal heterogeneity of the strain values was not taken into consideration, normal segments with lower strain values were classified as non-transmural MI (false positive), and thus the specificity of the classification of non-transmural MI was only 65% and 69%, when using peak systolic S_C and S_R, respectively (Table 1). Measuring the peak systolic S_C and S_R values relatively to normal values caused an increase of the correct classification of the non-transmural MI, and the specificity was increased to 84% and 79%, when using peak systolic S_C and S_R relative to normal values, respectively. It is important to mention that the peak systolic strain for each segment was measured relatively to the average normal value of 21 rats and not relatively to its own baseline value, which may allow a more general implementation of the technique. Such a sensitive regional analysis of the strain measurements was possible due to the utilization of a novel wavelet de-noising process, which was applied to the myocardial velocities after the speckle tracking, instead of the built-in smoothing process of the commercial STE program.

Detection of MI by STE was previously reported by Gjesdal et al., who analyzed the global longitudinal and circumferential strains of patients with chronic ischemic heart disease (Gjesdal et al., 2007, 2008). The detection of MI mass was found to be precise when by utilizing global longitudinal and circumferential strains (Gjesdal et al., 2008). However, in the present study, we propose to enhance the detection, specifically of non-transmural MI, by taking into consideration the normal segmental heterogeneity. The normal segmental heterogeneity of the longitudinal strain was studied by Marwick et al., who performed the measurements over 250 normal subjects (Marwick et al., 2009). Marwick et al. found peak systolic longitudinal strain of -13.7±4.0 % at the basal septum, while the global longitudinal strain value of -15.3±1.9% was considered by Gjesdal et al. as a value signifying a medium sized MI. Thus, normal segments with lower strain values might be

classified by mistake as an infarcted area. It is important to note that taking into consideration the heterogeneity of the normal values is relevant only if the heterogeneity is significant. The heterogeneity of the peak systolic S_C at the PM level is not statistically significant. Thus, taking into consideration the normal values influences only the measurement peak systolic S_C values of the AP level.

The detection of transmural MI does not require normalization to baseline. The strain values are severely reduced, and in some cases the myocardium even undergoes stretching instead of contraction during diastole, as seen in the transmural MI example in Fig. 2 and in the study of Migrino et al. (Migrino et al., 2007). In this study we found that the peak systolic S_C is a better detector of transmural MI than peak systolic S_R ($P<0.05$). Gjesdal et al. (Gjesdal et al., 2008)and Popović et al. (Popović et al., 2007)) also reported better detection of transmural MI by S_C than by S_R (Gjesdal et al., 2008); however Migrino et al. reported that S_R is a better predictor of transmural MI (Migrino et al., 2007, 2008). The S_R cannot be a better predictor of transmural MI since the STE commercial program contains stronger spatial smoothing at the radial direction than that at the circumferential direction. This phenomenon is demonstrated by comparing Figs. 2B and 2C in Popović et al. In their Fig. 2B there was heterogeneity in the segmental peak systolic S_C in normal and MI states. In contrast, no heterogeneity was seen by the S_R in Fig. 2C (Popović et al., 2007). The normal heterogeneity of the peak systolic S_R that was measured in our present study (Fig. 1C) can be seen by eyeballing the short-axis scans. Another influence of the smoothing process is the correlation between the strain at the MI areas and the non-MI areas. Migrino et al. reported a correlation of 0.82 between end systolic S_R of the MI and periinfarct areas. Moreover, they reported a correlation of 0.64 between end systolic S_R of the MI and remote areas (Migrino et al., 2008). These strong correlations, which occur due to the smoothing process of the commercial program, do not occur when using the wavelet de-noising process that we propose in this study. The correlation between the non-MI area and the MI area in this study was 0.24 for the S_C and 0.06 for the S_R at the PM level. This result demonstrates that the peak systolic S_R of the remote areas at 24 hours of reperfusion do not correlate to the MI size. This result was not surprising since a previous Doppler echocardiography study has already reported that remote areas can show normal contractility (Vartdal et al., 2007).

4.1 Study limitations

The main limitation of the wavelet de-noising process used here is its sensitivity to artifacts at the B-mode cines. The commercial program compensates for artifacts, such as areas in which the myocardium is shaded by the ribs (black area), by imposing there the averaged values. The wavelet de-noising shows no movement in these areas while the commercial program depicts normal movement. Thus, when applying the wavelet de-noising algorithm used here, it is important to include only ultrasound cines with good image quality.

5. Conclusions

Based on our results we concluded that in the rat model a natural heterogeneity among the strain values exists. Taking into consideration this normal heterogeneity, by measuring the

strains relatively to the normal values, improves the detection of non-transmural MI. This kind of measurement is particularly suitable for stress-echocardiography, which includes comparison of the echo results at stress to those at baseline, and is specified for the detection of minor ischemia.

In humans, this kind of study should be performed in the future by normalizing the longitudinal strain relative to baseline and not the circumferential strain as performed here, since the heterogeneity of the strain in humans mostly exists at the longitudinal direction from base to apex (Bachner-Hinenzon et al., 2010).

6. Acknowledgments

This work was supported by the Chief Scientist, the Ministry of Industry and Commerce Magneton project, the Technion VP for Research and the Alfred Mann Institute at the Technion (AMIT).

7. References

Bachner-Hinenzon N Ertracht O, Lysiansky M, Binah O, Adam D. Layer-specific assessment of left ventricular function by utilizing wavelet de-noising: A validation study. Med Biol Eng Comput. 2011 Jan;49(1):3-13. Epub 2010 Jul 20.

Bachner-Hinenzon N, Ertracht O, Leitman M, Vered Z, Shimoni S, Beeri R, Binah O, Adam D. Layer-specific strain analysis by speckle tracking echocardiography reveals differences in left ventricular function between rats and humans. Am J Physiol Heart Circ Physiol. 2010 Sep;299(3):H664-72. Epub 2010 Jul 2.

Bhindi R, Witting PK, McMahon AC, Khachigian LM, Lowe HC. Rat models of myocardial infarction. Pathogenetic insights and clinical relevance. Thromb Haemost. 96(5):602-10, 2006.Review.

Fu Q, Xie M, Wang J, Wang X, Lv Q, Lu X, Fang L, Chang L. Assessment of regional left ventricular myocardial function in rats after acute occlusion of left anterior descending artery by two-dimensional speckle tracking imaging. J Huazhong Univ Sci Technolog Med Sci. 29(6):786-90, 2009.

Gjesdal O, Helle-Valle T, Hopp E, Lunde K, Vartdal T, Aakhus S, Smith HJ, Ihlen H, Edvardsen T. Noninvasive separation of large, medium, and small myocardial infarcts in survivors of reperfused ST-elevation myocardial infarction: a comprehensive tissue Doppler and speckle-tracking echocardiography study. Circ Cardiovasc Imaging. 1(3):189-96, 2008.

Gjesdal O, Hopp E, Vartdal T, Lunde K, Helle-Valle T, Aakhus S, Smith HJ, Ihlen H, Edvardsen T. Global longitudinal strain measured by two-dimensional speckle tracking echocardiography is closely related to myocardial infarct size in chronic ischaemic heart disease. Clin Sci (Lond). 113(6):287-96, 2007.

Hale SL, Sesti C, Kloner RA. Administration of erythropoietin fails to improve long-term healing or cardiac function after myocardial infarction in the rat. J Cardiovasc Pharmacol. 46(2):211-5, 2005.

Leitman M, Lysyansky P, Sidenko S, Shir V, Peleg E, Binenbaum M, Kaluski E, Krakover R, Vered Z. Two-dimensional strain-a novel software for real-time quantitative

echocardiographic assessment of myocardial function. J Am Soc Echocardiogr. 17(10):1021-9, 2004.

Liel-Cohen N, Tsadok Y, Beeri R, Lysyansky P, Agmon Y, Feinberg MS, Fehske W, Gilon D, Hay I, Kuperstein R, Leitman M, Deutsch L, Rosenmann D, Sagie A, Shimoni S, Vaturi M, Friedman Z, Blondheim DS. A New Tool for Automatic Assessment of Segmental Wall Motion, Based on Longitudinal 2D Strain: A Multicenter Study by the Israeli Echocardiography Research Group. Circ Cardiovasc Imaging. 3(1):47-53, 2010.

Marwick TH, Leano RL, Brown J, Sun JP, Hoffmann R, Lysyansky P, Becker M, Thomas JD. Myocardial strain measurement with 2-dimensional speckle-tracking echocardiography: definition of normal range. JACC Cardiovasc Imaging. 2(1):80-4, 2009.

Migrino RQ, Zhu X, Morker M, Brahmbhatt T, Bright M, Zhao M. Myocardial dysfunction in the periinfarct and remote regions following anterior infarction in rats quantified by 2D radial strain echocardiography: an observational cohort study. Cardiovasc Ultrasound. 6:17, 2008.

Migrino RQ, Zhu X, Pajewski N, Brahmbhatt T, Hoffmann R, Zhao M. Assessment of segmental myocardial viability using regional 2-dimensional strain echocardiography. J Am Soc Echocardiogr. 20(4):342-51, 2007.

Notomi Y, Lysyansky P, Setser RM, Shiota T, Popovic ZB, Martin- Miklovic MG, Weaver JA, Oryszak SJ, Greenberg NL, White RD, Thomas JD. Measurement of ventricular torsion by two-dimensional ultrasound speckle tracking imaging. J. Am. Coll. Cardiol. 45: 2034–2041, 2005.

Ojha N, Roy S, Radtke J, Simonetti O, Gnyawali S, Zweier JL, Kuppusamy P, Sen CK. Characterization of the structural and functional changes in the myocardium following focal ischemia-reperfusion injury. Am J Physiol Heart Circ Physiol. 294(6):H2435-43, 2008.

Picano E, Lattanzi F, Orlandini A, Marini C, L'Abbate A. Stress echocardiography and the human factor: the importance of being expert. J Am Coll Cardiol. 17(3):666-9, 1991.

Pitts KR, Stiko A, Buetow B, Lott F, Guo P, Virca D, Toombs CF. Washout of heme-containing proteins dramatically improves tetrazolium-based infarct staining. J Pharmacol Toxicol Methods. 55(2):201-8, 2007.

Popović ZB, Benejam C, Bian J, Mal N, Drinko J, Lee K, Forudi F, Reeg R, Greenberg NL, Thomas JD, Penn MS. Speckle-tracking echocardiography correctly identifies segmental left ventricular dysfunction induced by scarring in a rat model of myocardial infarction. Am J Physiol Heart Circ Physiol. 292(6):H2809-16, 2007.

Rappaport D, Adam D, Lysyansky P, Riesner S. Assessment of myocardial Regional Strain and Strain Rate by Tissue Tracking in B-Mode Echocardiograms. Ultrasound in Med. & Biol., 32(8): 1181–1192, 2006.

Reinhardt CP, Weinstein H, Wironen J, Leppo JA. Effect of triphenyl tetrazolium chloride staining on the distribution of radiolabeled pharmaceuticals. J Nucl Med. 34(10):1722-7, 1993.

Reisner SA , Lysyansky P, Agmon Y, Mutlak D, Lessick J, Friedman Z. Global longitudinal strain: a novel index of left ventricular systolic function. J. Am. Soc. Echocardiogr. 17(6): 630-633. 2004.

Schiller NB, Shah PM, Crawford M, DeMaria A, Devereux R, Feigenbaum H, Gutgesell H, Reichek N, Sahn D, Schnittger I, et al. Recommendations for quantitation of the left ventricle by two-dimensional echocardiography. American Society of Echocardiography Committee on Standards, Subcommittee on Quantitation of Two-Dimensional Echocardiograms. J Am Soc Echocardiogr. 2(5):358-67, 1989.

Vartdal T, Brunvand H, Pettersen E, Smith HJ, Lyseggen E, Helle-Valle T, Skulstad H, Ihlen H, Edvardsen T. Early prediction of infarct size by strain Doppler echocardiography after coronary reperfusion. J Am Coll Cardiol. 24;49(16):1715-, 2007.

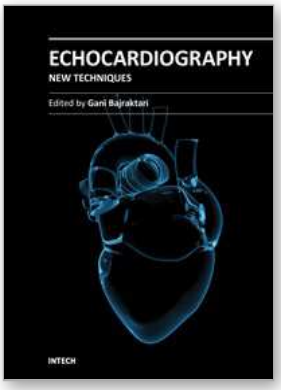

Echocardiography - New Techniques

Edited by Prof. Gani Bajraktari

ISBN 978-953-307-762-8
Hard cover, 218 pages
Publisher InTech
Published online 18, January, 2012
Published in print edition January, 2012

The book "Echocardiography - New Techniques" brings worldwide contributions from highly acclaimed clinical and imaging science investigators, and representatives from academic medical centers. Each chapter is designed and written to be accessible to those with a basic knowledge of echocardiography. Additionally, the chapters are meant to be stimulating and educational to the experts and investigators in the field of echocardiography. This book is aimed primarily at cardiology fellows on their basic echocardiography rotation, fellows in general internal medicine, radiology and emergency medicine, and experts in the arena of echocardiography. Over the last few decades, the rate of technological advancements has developed dramatically, resulting in new techniques and improved echocardiographic imaging. The authors of this book focused on presenting the most advanced techniques useful in today's research and in daily clinical practice. These advanced techniques are utilized in the detection of different cardiac pathologies in patients, in contributing to their clinical decision, as well as follow-up and outcome predictions. In addition to the advanced techniques covered, this book expounds upon several special pathologies with respect to the functions of echocardiography.

InTech Europe
University Campus STeP Ri
Slavka Krautzeka 83/A
51000 Rijeka, Croatia
Phone: +385 (51) 770 447
Fax: +385 (51) 686 166
www.intechopen.com

InTech China
Unit 405, Office Block, Hotel Equatorial Shanghai
No.65, Yan An Road (West), Shanghai, 200040, China
中国上海市延安西路65号上海国际贵都大饭店办公楼405单元
Phone: +86-21-62489820
Fax: +86-21-62489821